

# Elevated Intraocular Pressure, Optic Nerve Atrophy, and Impaired Retinal Development in ODAG Transgenic Mice

Takaaki Sasaki,<sup>1,2</sup> Wataru Watanabe,<sup>1,2</sup> Yuki Muranishi,<sup>3</sup> Takashi Kanamoto,<sup>2</sup> Makoto Aihara,<sup>4</sup> Kazuko Miyazaki,<sup>1</sup> Hiroki Tamura,<sup>2</sup> Tadashi Saeki,<sup>4</sup> Hideaki Oda,<sup>5</sup> Nazariy Souchelnytskyi,<sup>6</sup> Serbiy Souchelnytskyi,<sup>6</sup> Hirohiko Aoyama,<sup>7</sup> Zen-ichiro Honda,<sup>8</sup> Takabisa Furukawa,<sup>3</sup> Hiromu K. Mishima,<sup>9</sup> Yoshiaki Kiuchi,<sup>2</sup> and Hiroaki Honda<sup>1</sup>

**PURPOSE.** In an earlier study, a cDNA was cloned that showed abundant expression in the eye at postnatal day (P)2 but was downregulated at P10; it was named *ODAG* (ocular development-associated gene). Its biological function was examined by generating and analyzing transgenic mice overexpressing ODAG (ODAG Tg) in the eye and by identifying ODAG-binding proteins.

**METHODS.** Transgenic mice were generated by using the mouse *Crx* promoter. EGFP was designed to be coexpressed with transgenic ODAG, to identify transgene-expressing cells. Overexpression of ODAG was confirmed by Northern and Western blot analysis. IOP was measured with a microneedle technique. The eyes were macroscopically examined and histologically analyzed. EGFP expression was detected by confocal microscope. Proteins associated with ODAG were isolated by pull-down assay in conjugation with mass spectrometry.

**RESULTS.** Macroscopically, ODAG Tg exhibited gradual protrusion of the eyeballs. The mean IOP of ODAG Tg was significantly higher than that of wild-type (WT) littermates. Histologic analysis exhibited optic nerve atrophy and impaired retinal development in the ODAG Tg eye. EGFP was expressed highly in the presumptive outer nuclear layer and weakly in the presumptive inner nuclear layer in the ODAG Tg retina. Rab6-GTPase-activating protein (Rab6-GAP) and its substrate, Rab6, were identified as ODAG-binding proteins.

**CONCLUSIONS.** Deregulated expression of ODAG in the eye induces elevated intraocular pressure and optic nerve atrophy and impairs retinal development, possibly by interfering with the Rab6/Rab6-GAP-mediated signaling pathway. These results provide new insights into the mechanisms regulating ocular development, and ODAG Tg would be a novel animal model for human diseases caused by ocular hypertension. (*Invest Ophthalmol Vis Sci.* 2009;50:242-248) DOI:10.1167/iovs.08-2206

Ocular development is a complex process, involving several genes with expression that is strictly controlled in a spatial and temporal manner. Although several genes, including *Pax6*, *Rx*, and *Crx*, are essential for normal ocular formation,<sup>1-3</sup> the molecular mechanism(s) governing eye development has not been fully elucidated.

To identify genes that are preferentially expressed in the developing eye, we performed a differential display using mRNAs extracted from postnatal day (P)2 and P10 mouse eyes.<sup>4</sup> As a result, we isolated a cDNA fragment that had high expression in the eye at P2 but was downregulated at P10 and named it *ODAG* (ocular development-associated gene).<sup>4</sup> The *ODAG* gene product is composed of 266 amino acids and contains a putative zinc finger domain at the N-terminus.<sup>4</sup> In situ hybridization in the eye has revealed that *ODAG* mRNA is expressed in various regions, including the lens, ciliary body, retina, sclera, and conjunctiva, but its expression level in the retina attenuates with growth.<sup>4</sup> At P2, *ODAG* was highly expressed in all the retinal layers (presumptive outer nuclear layer [ONL], presumptive inner nuclear layer [INL], and ganglion cell layer [GCL]), but at P7, its expression decreases, especially in the GCL, and at P14, no apparent expression is detected.<sup>4</sup> These results strongly suggest that physiologically controlled *ODAG* expression in the eye would play an important role in normal ocular development, but its biological function remains unknown.

To investigate, we generated transgenic mice overexpressing ODAG (ODAG Tg). The mouse *Crx* promoter, which directs transgene expression in photoreceptors,<sup>5,6</sup> was chosen as a regulatory element, and *IRE5/EGFP* was attached to the *ODAG* coding region as a reporter gene, to detect transgenic *ODAG*-expressing cells. Macroscopically, ODAG Tg exhibited gradual eye protrusion with increased intraocular pressure. Histologic examination of the ODAG Tg eye revealed optic nerve atrophy and retinal dysplasia. Analysis of EGFP expression demonstrated that transgenic ODAG was expressed highly in the presumptive ONL and weakly in the presumptive INL in the developing retina. In addition, by a pull-down assay using GST-ODAG conjugated with mass spectrometry, we identified Rab6-GAP and its substrate, Rab6, as ODAG-binding proteins. These results demonstrated that physiologically regulated ODAG expression is essential for normal eye development, possibly through a Rab6/Rab6-GAP-mediated pathway.

From the <sup>1</sup>Department of Developmental Biology, Research Institute for Radiation Biology and Medicine, the Departments of <sup>2</sup>Ophthalmology and Visual Science and <sup>7</sup>Anatomy, Graduate School of Biomedical Sciences, Hiroshima University, Hiroshima, Japan; <sup>3</sup>The 4th Department, Osaka Bioscience Institute, Osaka, Japan; the Departments of <sup>4</sup>Ophthalmology and <sup>8</sup>Allergy and Rheumatology, Graduate School of Medicine, University of Tokyo, Tokyo, Japan; the <sup>5</sup>Department of Pathology, Tokyo Women's Medical University, Tokyo, Japan; the <sup>6</sup>Ludwig Institute for Cancer Research, Uppsala, Sweden; and the <sup>9</sup>Hiroshima General Hospital of West Japan Railway Company, Hiroshima, Japan.

Supported in part by a Grant-in-Aid from the Ministry of Education, Science and Culture of Japan and the Ryokufukai Foundation.

Submitted for publication April 22, 2008; revised August 5, 2008; accepted October 28, 2008.

Disclosure: T. Sasaki, None; W. Watanabe, None; Y. Muranishi, None; T. Kanamoto, None; M. Aihara, None; K. Miyazaki, None; H. Tamura, None; T. Saeki, None; H. Oda, None; N. Souchelnytskyi, None; S. Souchelnytskyi, None; H. Aoyama, None; Z. Honda, None; T. Furukawa, None; H.K. Mishima, None; Y. Kiuchi, None; H. Honda, None

The publication costs of this article were defrayed in part by page charge payment. This article must therefore be marked "advertisement" in accordance with 18 U.S.C. §1734 solely to indicate this fact.

Corresponding author: Hiroaki Honda, Department of Developmental Biology, Research Institute for Radiation Biology and Medicine, Hiroshima University, 1-2-3 Kasumi, Minami-ku, Hiroshima 734-8553 Japan; hhonda@hiroshima-u.ac.jp.

## MATERIALS AND METHODS

### Construction of the Transgene and Generation of Transgenic Mice

The mouse *Crx* promoter (~12 kb) was excised from a *pCrx12K*-transgenic cassette<sup>5</sup> with *NotI* and *PmeI* and subcloned into the *NotI*-*EcoRV* sites of a phagemid (pBluescript; *pCrx12K/pBS*; Stratagene, Tokyo, Japan). The coding region of mouse *ODAG* cDNA was amplified with 5' (5'-TCTTCCAAAGGTGCCCTCA-3') and 3' (5'-CCAGAAA-GAGTGATTCCGCT-3') primers by using mouse *ODAG* cDNA, as described elsewhere.<sup>4,7</sup> A DNA fragment of the expected size was subcloned into the *PCR-Blunt II-TOPO* cloning vector (Invitrogen, Tokyo, Japan), and correct amplification was verified by sequencing. The *ODAG* coding region was excised with *XbaI* and *SpeI*, blunt-ended by Klenow enzyme (Takara Shuzo, Kyoto, Japan), and subcloned into the *EcoRV* site of an *IRES/EGFP/pA* vector, which contains *IRES* (internal ribosomal entry site)/*EGFP* (enhanced green fluorescent protein) (derived from *pIRES2-EGFP*; BD-Clontech Laboratories, Inc., Palo Alto, CA) and *SV40* splicing and *polyA(pA)* signals<sup>8</sup> downstream of the cloning sites. A fragment containing the *ODAG* coding region, *IRES/EGFP*, and *SV40* splicing and *pA* signals was excised with *XbaI* and *SacII*, blunt-ended by T4 DNA polymerase (Takara Shuzo), and subcloned into the *HinII* site of *pCrx12K/pBS*, which was located downstream of the mouse *Crx* promoter. A *NotI*-digested fragment containing the mouse *Crx* promoter, mouse *ODAG* coding region, *IRES/EGFP*, and *SV40* splicing and *pA* signals was excised, purified, and microinjected into the pronuclei of fertilized eggs of BDF2 mice, as previously described.<sup>8</sup> Founder mice and their transgenic progeny were identified by Southern blot analysis, using *ODAG* cDNA as a probe.<sup>8</sup> All the mice were kept according to the guidelines of the Institute of Laboratory Animal Science, Hiroshima University, and the protocol complied with the ARVO Statement for the Use of Animals in Ophthalmic and Vision Research.

### Histologic Examination and Detection of EGFP-Expressing Cells

Histologic analysis was performed essentially as previously described.<sup>8</sup> In brief, mouse eyeballs from anesthetized mice were fixed in 10% formalin, cut in 4- $\mu$ m sections, stained with hematoxylin and eosin (HE), and examined under a light microscope. For detecting EGFP expression in the retina, retinas dissected from eyeballs were placed in PBS and were examined under a stereomicroscope (SterEO Lumar.V12 microscope; Carl Zeiss Meditec, Tokyo, Japan). To identify EGFP-expressing cells in the retinal layers, the retinas were fixed in 4% paraformaldehyde in 0.1 M phosphate buffer (pH 7.4), rinsed in phosphate buffer, and equilibrated in 30% sucrose/PBS overnight at 4°C. They were then embedded in optimal cutting temperature (OCT) compound and frozen at -20°C. Frozen blocks were sectioned at 20- $\mu$ m thickness with a cryostat (Cryostar HM 560 MV; Carl Zeiss Meditec), washed in PBS, and mounted with mounting medium. Digital images were acquired on a confocal microscope (Axiovert 100M; Carl Zeiss Meditec) and processed by graphics software (LSM 510 ver. 3.0 software; Carl Zeiss Meditec).

### Intraocular Pressure Measurement

IOP was measured by using a microneedle technique.<sup>9</sup> In brief, after mice were anesthetized with 100  $\mu$ g/kg of ketamine and 9  $\mu$ g/kg of xylazine, the tip of a microneedle was inserted into the anterior chamber through the cornea, and the released pressure was transferred to a transducer that measured the IOP. The mean IOPs of ODAG Tg and WT were compared by using Student's *t*-test.

### Northern Blot Analysis

Total RNA was prepared from whole eyes (Isogen; Invitrogen), electrophoresed in 1% agarose gel containing 37% formaldehyde, transferred to a membrane (Hybond-N; GE Healthcare, Tokyo, Japan), and

hybridized with <sup>32</sup>P-dCTP-labeled *ODAG* cDNA or *GAPDH* as a probe. Positive signals were detected by a phosphoimage analyzer (Fuji X Bas2000; Fujifilm, Tokyo, Japan).

### Western Blot Analysis

Western blot analysis was performed as previously described.<sup>10</sup> In brief, cell lysates were extracted in lysis buffer (150 mM NaCl, 20 mM Tris-HCl [pH 7.4], 1% Triton-X, 0.5% deoxycholate, 1 mM phenylmethylsulfonyl fluoride, 10 mM NaF, and 20 mg/mL aprotinin). Protein aliquots were separated by SDS-PAGE, transferred to a nitrocellulose membrane (Hybond-C; GE Healthcare), blocked with 5% skim milk in TBST buffer (10 mM Tris-HCl [pH 7.4], 150 mM NaCl, and 0.1% Tween-20), and incubated with an anti-ODAG polyclonal antibody that was raised against a peptide, WTHVGPTPAITIKETVANHL, that corresponds to the C-terminal region of the mouse ODAG protein (1:1000; Kurabo Co., Ltd., Osaka, Japan) or an anti-Rab6 antibody (1:500; Santa Cruz Biotechnology, Santa Cruz, CA). The blots were developed by enhanced chemiluminescence (ECL; GE Healthcare).

### GST Pull-Down Assay

To purify a recombinant ODAG protein, we inserted the coding region of *ODAG* cDNA into the *EcoRI*-*XbaI* sites of the pGEX4T1 vector (BD Biosciences, Piscataway, NJ) and introduced into the BL21 bacterial cells. Expression of the glutathione-S-transferase (GST)-ODAG fusion protein (GST-ODAG) or GST alone was induced by addition of 1 mM isopropyl- $\beta$ -D-thiogalactopyranoside (IPTG; Sigma-Aldrich, St. Louis, MO). Bacterial cells were lysed in PBS containing 1% Triton X-100, and the recombinant protein was collected using Sepharose 4B (GE Healthcare) and eluted with elution buffer (10 mM glutathione and 50 mM Tris-HCl [pH 8.0]). Whole-cell extracts of R28 retinal precursor cells were incubated with GST-ODAG or GST alone, and the bound proteins were collected on glutathione-Sepharose, as previously described.<sup>11</sup>

### Two-Dimensional Electrophoresis and Protein Identification

Two-dimensional electrophoresis and protein identification were performed as previously described.<sup>12</sup> In brief, proteins precipitated with GST-ODAG and GST alone were solubilized in sample buffer (8 M urea, 4% CHAPS, 0.5% dithiothreitol [DTT], and IPG [pH 3-10]). Samples were applied by in-gel rehydration to a strip with immobilized pH gradient (pH 3-10, nonlinear gradient, 18 cm; GE Healthcare). First-dimension isoelectrophoresis was performed (IPGphor; GE Healthcare). A strip was equilibrated and placed on 10% SDS-PAGE. After SDS-PAGE electrophoresis, the gels were stained with silver nitrate. Silver nitrate-stained protein spots were scanned (Epson, Nagano, Japan) and analyzed (PD-Quest software; Bio-Rad, Tokyo, Japan). Protein spots of interest were directly excised and subjected to in-gel digestion with trypsin. Spectra were obtained (MALDI-TOF-MS; Bruker Daltonics, Billerica, MA) and a database search (NCBIInr, Matrix Science Ltd., Tokyo, Japan; using the ProFound protein search engine available at <http://prowl.rockefeller.edu/prowl-cgi/profound.exe>; developed by W. Zhang and B. T. Chait and provided in the public domain by Rockefeller University, New York, NY) was used for identification of protein names.

### Generation of ODAG-EGFP Fusion Protein

To generate the *ODAG-EGFP* fusion construct, the mouse *ODAG* coding region was amplified with 5' (5'-GAATCCACCACATGCCGCTGGGCTGAAGC-3') and 3' (5'-GGATCCCGCAAGTGGTTGGCAACTGTTTCC-3') primers, where the bold nucleotide was substituted to match Kozak's rule and the italic nucleotides were added to create restriction enzyme sites. The amplified fragment was digested with *EcoRI* and *BamHI* (Takara Shuzo) and subcloned into the *EcoRI*-*BamHI* sites of an expression vector, pEGFP-N1 (BD-Clontech), where the *ODAG* coding region and *EGFP* cDNA were fused in-frame and placed downstream of the cytomegalovirus promoter. Correct ampli-

fication of the *ODAG* coding region and its in-frame fusion to *EGFP* cDNA were verified by sequencing.

## DNA Transfection

COS-7 cells were seeded at a density of  $3 \times 10^5$  in a 60-mm<sup>2</sup> tissue culture dish at least 24 hours before transfection. On the next day, when the cells reached 50% to 60% confluence, they were transfected with 2  $\mu$ g of ODAG-EGFP expression plasmid (4  $\mu$ L of FuGENE 6; Roche Molecular Biochemicals, Indianapolis, IN) according to the manufacturer's instructions. Twelve to 48 hours after transfection, living cells were observed under a fluorescence microscope (BioZero BZ-8000; Keyence, Osaka, Japan).

## RESULTS

### Generation of ODAG Tg and Overexpression of ODAG in the Transgenic Eye

We planned to generate transgenic mice overexpressing ODAG in the eye. For this purpose, we used mouse *Crx* promoter that directs transgene expression in photoreceptor cells<sup>5,6</sup> as a regulatory element and to detect transgene-expressing cells, *IRES/EGFP* was placed after the *ODAG* coding region (Fig. 1A). From this transgene, a single mRNA containing the *ODAG* coding region and *IRES/EGFP* (larger than the endogenous *ODAG* message) was generated by the *Crx* promoter, whereas two different proteins, ODAG (the same molecular weight as the endogenous one) and EGFP, were produced by the *Crx* promoter in combination with the *IRES* (Fig. 1A). Three independent transgenic lines containing approximately 5 to 10 copies of the transgene were established, and all the lines showed similar transgene expression levels and almost the same phenotype (data not shown).

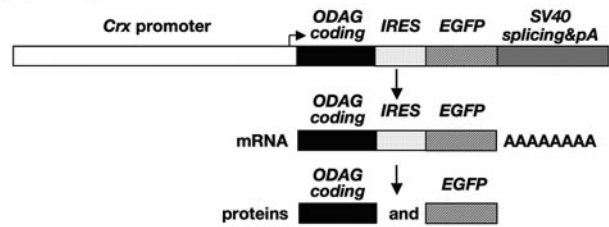
To examine the overexpression of *ODAG* in the transgenic eye, we subjected RNAs extracted from eyes of ODAG Tg and WT littermates to Northern blot analysis with *ODAG* cDNA used as a probe. The results show that the transgenic eye expressed a high amount of exogenous *ODAG* mRNA (Fig. 1B, arrow) in addition to endogenous *ODAG* mRNA (Fig. 1B, arrowhead). To confirm the overexpression of ODAG at the protein level, we generated a polyclonal antibody against C-terminal peptides of ODAG and performed a Western blot analysis. ODAG protein was abundantly expressed in the transgenic eye compared with the WT eye (Fig. 1C, arrow). These results indicate that ODAG Tg overexpressed ODAG mRNA and protein in the eye.

### Eye Protrusion with High IOP in ODAG Tg

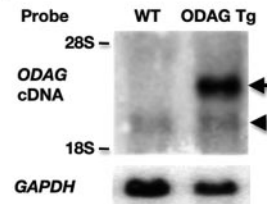
At birth, the eyes of the ODAG Tg were macroscopically indistinguishable from those of WT. However, at 7 to 8 weeks of age, exophthalmos appeared in all the ODAG Tg and progressed and developed into megalocornea-like buphthalmos (Fig. 2A, arrows, top right). The surfaces of the extended corneas of ODAG Tg became turbid and opaque, and infiltration of neovessels into the corneas was occasionally observed (Fig. 2A; bottom right, arrows and an arrowhead).

We then measured IOPs in the ODAG Tg and compared them to those of the WT (7–11 weeks of age). The results indicate that the IOPs of the ODAG Tg were significantly higher than those in the WT. The IOPs of the ODAG Tg ( $n = 30$  eyes) were  $24.02 \pm 7.35$  mm Hg, with maximum and minimum IOPs being 41.78 and 8.77 mm Hg, respectively. Among them, 5 mice exhibited extremely high IOP ( $>30$  mm Hg), 10 mice showed high IOP ( $>20$  mm Hg), and only 1 mouse had normal IOP ( $<20$  mm Hg). In contrast, IOPs of WT mice ( $n = 30$  eyes) were  $15.87 \pm 1.45$  mm Hg, with maximum and minimum IOPs being 19.22 and 13.57 mm Hg, respec-

### (A) transgene structure



### (B) Northern blot



### (C) Western blot

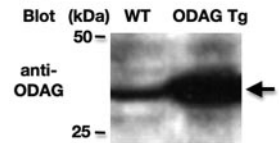


**FIGURE 1.** Generation of ODAG Tg and expression of ODAG in the eye. (A) The transgene and its transcribed and translated products. It is composed of the mouse *Crx* promoter, the *ODAG* coding region, the internal ribosomal entry site (*IRES*), enhanced green fluorescent protein (*EGFP*), and *SV40* splicing and polyadenylation (*polyA*) signals. From this transgene, a single mRNA containing the *ODAG* coding region and *IRES/EGFP* is generated, and two different proteins, ODAG and EGFP, are produced. (B) Northern blot for *ODAG* mRNA expression in the eye. mRNAs extracted from WT and ODAG Tg were hybridized with mouse *ODAG* cDNA (*top*) or *GAPDH* (*bottom*) as a probe. Endogenous (*arrowhead*) and transgene-derived *ODAG* (*arrow*) mRNAs. (C) Western blot analysis for ODAG protein expression in the eye. Whole-cell extracts from eyes of WT and ODAG Tg were separated by SDS-PAGE, transferred to a nylon membrane, and probed with an anti-ODAG antibody. *Arrow*: the position of ODAG protein.

tively. The mean IOPs of both groups are shown in Figure 2B with error bars; the difference between the two groups was statistically significant ( $P < 0.01$ ).

### Optic Nerve Atrophy and Impaired Retinal Development in ODAG Tg

To investigate neuronal abnormalities in the ODAG Tg, the optic nerve (ON) was examined. Macroscopically, the ONs of the ODAG Tg were very thin and small compared with those of the WT (Fig. 3A, top). Histologic examination showed that the ONs of ODAG Tg were hypoplastic and contained fewer retinal nerve fibers than those of the WT (Fig. 3A, bottom). In addition, optic discs of the ODAG Tg were poorly formed and difficult to detect (data not shown).

To investigate intraocular changes, we subjected the eye specimens of the ODAG Tg and WT to HE staining. Under low magnification, the ODAG Tg eye specimen exhibited thin retinal layers and extended cornea (Fig. 3B, top, black and white triangles). Examination with high magnification revealed that, although the basic structures were retained in the retina of the ODAG Tg, all the cell layers were poorly developed, irregularly arranged, and contained fewer cells than those of the WT (Fig. 3B, middle). In some of the ODAG Tg samples, only a single intraretinal nuclear layer was formed, instead of separate INL and ONL (Supplementary Fig. S1, <http://www.iovs.org/cgi/content/full/50/1/242/DC1>).

We then examined the anterior chamber angle to see whether the high IOPs in the ODAG Tg are caused by a closed angle. The results showed that the angle of the anterior chamber was open in the ODAG Tg as well as the WT (Fig. 3B, bottom, arrows), indicating that the ocular hypertension in ODAG Tg was not attributable to angle closure.

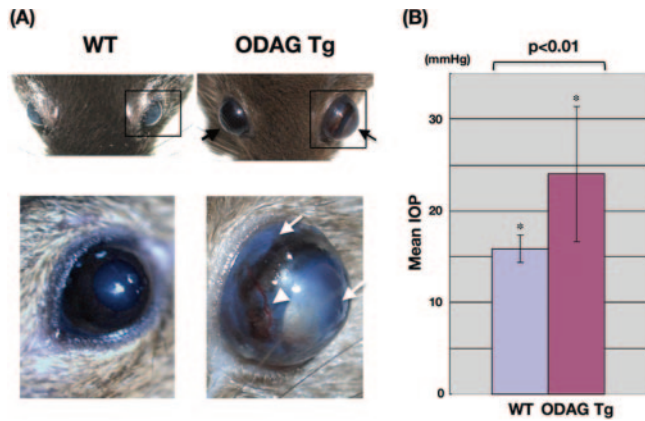


**FIGURE 2.** Macroscopic eye appearances and mean IOP of WT and ODAG Tg. (A) External eye appearances of WT (*left*) and ODAG Tg (*right*) at 9 weeks of age. Boxed areas in the *top* panels are magnified in the *bottom* panels. Note the enlarged eyeballs (indicated by *arrows*, *top right*) and turbid and opaque cornea with neovessel infiltration (indicated by *arrows*, *arrowhead*, respectively, *bottom right*) in ODAG Tg sections. (B) Comparison of IOPs between WT and ODAG Tg from 7 to 11 weeks of age. The mean results of total 30 WT and ODAG Tg (10 WT and ODAG Tg from each transgenic line) are shown with  $\pm$ SD. The difference between the mean IOPs of WT and ODAG Tg is statistically significant ( $P < 0.01$ , Student's *t*-test).

**Expression of Transgenic ODAG in the Presumptive INL and ONL in the Developing Retina**

To investigate the mechanism underlying the impaired retinal development observed in the ODAG Tg, we attempted to detect transgene-expressing cells in the retina. Since *IRES/*

*EGFP* was attached to the *ODAG* coding region in the transgene (Fig. 1A), *EGFP* should have coexpressed with transgenic *ODAG*. To examine whether *EGFP* expression could be detected in the retina, we observed whole retinas of WT and ODAG Tg under a fluorescence microscope at P6, when the *Crx* promoter drives high transgene expression.<sup>6</sup> Green fluorescence was clearly detected in the ODAG Tg retinas (Fig. 4A, right bottom), whereas no signal was observed in the WT retinas (Fig. 4A, bottom left), indicating that transgenic *ODAG*-expressing cells could be identified as *EGFP*-positive cells at this stage. To identify which cells in the retinal layers expressed *EGFP*, we observed retinal sections of the WT and ODAG Tg eyes under a confocal microscope. Among three retinal layers at P6 (presumptive ONL, presumptive INL, and GCL) in the ODAG Tg specimens, strong signal was detected in the presumptive ONL and weak signal was observed in the presumptive INL, whereas no positive signal was found in the GCL (Fig. 4B, bottom right), which contrasted with the WT retina, which exhibited only autofluorescence (Fig. 4B, bottom left). These results indicate that transgenic *ODAG* was highly expressed in the presumptive ONL, weakly expressed in the presumptive INL, but not expressed in GCL in the developing retina.

**Identification of Rab6-GAP and Rab6 as Recombinant ODAG-Binding Proteins**

We finally investigated molecules involved in the *ODAG*-mediated signaling pathway, by isolating protein(s) that forms a complex with *ODAG* by a GST pull-down assay in combination with proteomics. We generated a GST-fused *ODAG* protein (GST-*ODAG*) and confirmed its purity by SDS-PAGE (Fig. 5A, left lane). GST alone was used as a negative control (Fig. 5A, right lane). After these proteins were incubated with whole-

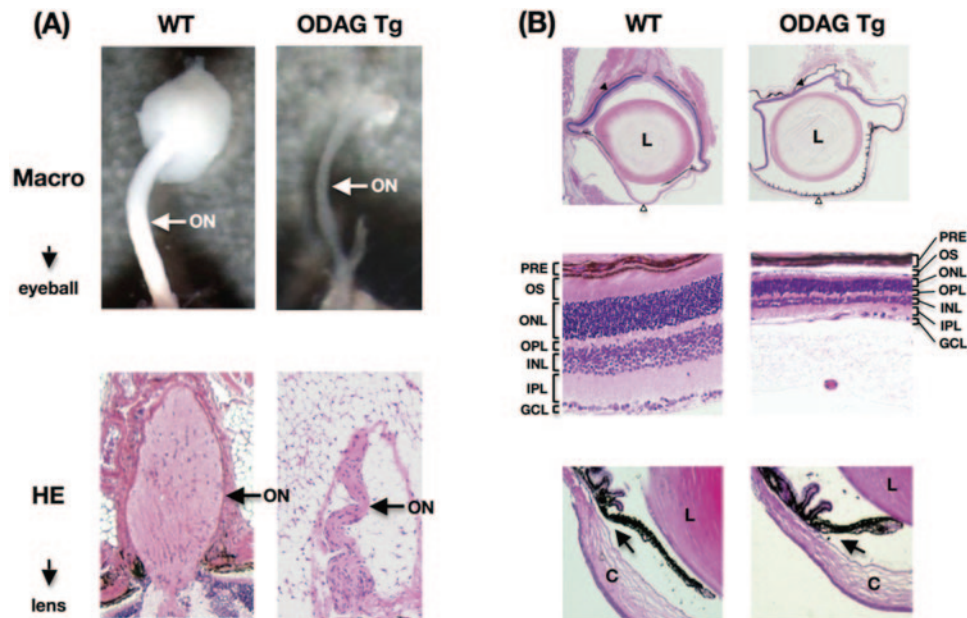


**FIGURE 3.** Pathologic analysis of WT and ODAG Tg eyes at 9 to 12 weeks of age. (A) Macroscopic (*top*) and HE-stained (*bottom*) optic nerves of WT (*left*) and ODAG Tg (*right*). The optic nerve of ODAG Tg is poorly developed (*top*) and contains few retinal nerve fibers (*bottom*) compared with that of WT. ON, optic nerve. (B) HE-stained eye sections of WT (*left*) and ODAG Tg (*right*). *Top*: whole-eye sections. (▲) The retinal layers and (Δ) cornea. Note the thin retinal layers and extended cornea in ODAG Tg. *Middle*: retinal sections. In contrast to the retinal layers in WT that were well differentiated and clearly divided, those of ODAG Tg were poorly developed and irregularly shaped and contained a small number of cells. RPE, retinal pigment epithelial layer; OS, outer segment; ONL, outer nuclear layer; OPL, outer plexiform layer; INL, inner nuclear layer; IPL, inner plexiform layer; GCL, ganglion cell layer. Lower panels: anterior chamber angles. In both WT and ODAG Tg eyes, the angles were open (*arrows*). L, lens; C, cornea.

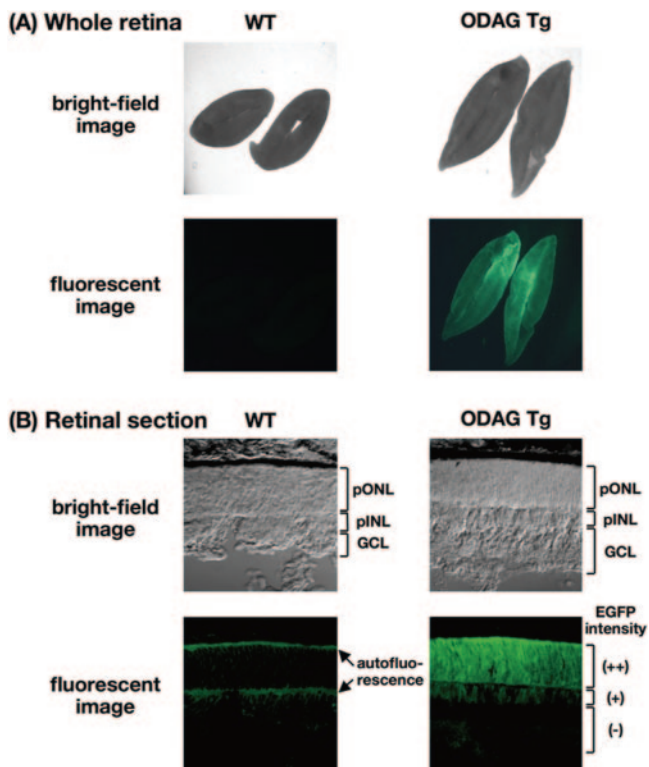


**FIGURE 4.** EGFP expression in the retinas of WT and ODAG Tg at P6. (A) EGFP expression in the whole retinas. Retinas were dissected from eye specimens of WT and ODAG Tg at P6 and observed with a fluorescence microscope. Bright-field and fluorescent images are shown. ODAG Tg retinas showed green fluorescence (*bottom right*), whereas no signal was observed in WT retinas (*bottom left*). (B) EGFP expression in the retinal layers. Retinal sections of WT and ODAG Tg eyes at P6 were observed with a confocal microscope. In the ODAG Tg section (*bottom right*), strong signal (++) was detected in the presumptive ONL (pONL), weak signal (+) in the presumptive INL (pINL), and no positive signal (-) in the GCL. *Bottom left*: autofluorescence in a WT section (*arrows*).

cell extracts of R28 rat retinal precursor cells,<sup>13</sup> binding proteins with GST-ODAG or GST alone were resolved by two-dimensional gel electrophoresis and the protein maps were compared. We used R28 cells for this assay, since it has been used for many ophthalmic examinations<sup>14</sup> and was found to express ODAG at a high level (data not shown). In four independent experiments, protein spots reproducibly detected only in GST-ODAG pull-down samples (Fig. 5B, arrow and dotted circles) were further analyzed by mass spectrometry. These spots were identified as rat Rab6-GTPase-activating protein (Rab6-GAP, NCBI ID: XP222799.2, pI: 5.1, 94.38 kDa) with high probability ( $P = 9.7e-0.01$ ; estimated  $z = 0.66$ ; sequence coverage, 13%). To investigate the possibility that GST-ODAG may also bind to Rab6, the substrate of Rab6-GAP, we performed a GST pull-down/Western blot analysis. The lysates of R28 cells were incubated with GST-ODAG or GST alone, and the bound proteins were analyzed by Western blot with an antibody against Rab6. The results show that Rab6 was included in the binding proteins of GST-ODAG (Fig. 5C), indicating that not only Rab6-GAP but also Rab6 was an ODAG-associated protein.

## DISCUSSION

Glaucoma is one of the most commonly observed disorders in the ophthalmic field, and elevated IOP is the major risk and

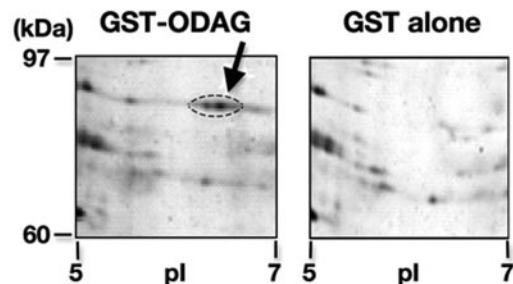
causative factor for glaucomatous optic neuropathy. Attempts have been made to develop animal models that replicate the clinical features of the disease and several mouse models with elevated IOP have been reported.<sup>15</sup> DBA/2 is a model of secondary open-angle glaucoma<sup>16,17</sup> and its substrain DBA/2NNia is used as a secondary closed-angle glaucoma model.<sup>18</sup> In addition, mice with a mutation in the collagen type-1 gene, which renders the gene product resistant to matrix metalloproteinase-mediated protein cleavage, are used as a model for open-angle glaucoma.<sup>19</sup> These models provide insights into the molecular mechanisms underlying disease development and also help in designing novel therapies for the disease.

In this study, we generated transgenic mice overexpressing ODAG in the eye and showed that the ODAG Tg exhibited gradual eye dilation with ocular hypertension, optic nerve atrophy, and impaired retinal development. The macroscopically apparent aspect was gradual eye protrusion with high ocular pressure, which resembled that of human congenital glaucoma. However, in contrast to the fact that high IOP in

## (A) Coomassie staining



## (B) Two-dimensional analysis



## (C) GST pull-down/Western blot

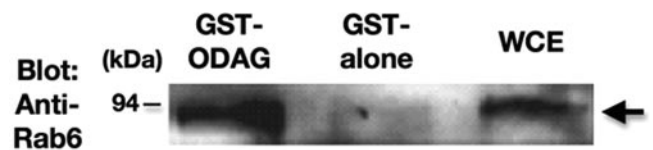


**FIGURE 5.** Interaction of Rab6-GAP and Rab6 with recombinant ODAG. (A) Purity of recombinant GST-ODAG fusion protein (GST-ODAG) and GST (GST alone) used for the pull-down assay. Both GST-ODAG and GST were seen as a single band by SDS-PAGE. (B) Result of two-dimensional gel analysis. The cell extracts of R28 cells were incubated with GST-ODAG or GST alone and proteins bound to GST-ODAG or GST alone were separated in a two-dimensional gel and stained with silver nitrate. *Dotted circle with arrow*: protein spots specific to GST-ODAG, which are identified as Rab6-GAP. (C) Association of GST-ODAG with Rab6. Pulled-down proteins with GST-ODAG or GST alone in R28 cell lysates were blotted with an anti-Rab6 antibody. Whole-cell extracts (WCE) of R28 cells were also loaded to show the position of Rab6 (*arrow*).

human congenital glaucoma is caused by a closed angle, pathologic analysis using HE-stained specimens and physiological examination using a gonioscope disclosed that the angle was open in ODAG Tg (Fig. 3B and not shown). The latter two abnormalities can be secondarily caused by consistent ocular hypertension. However, this was not the case in ODAG Tg, since these abnormalities already existed at 3 weeks of age, when corneal protrusion or high ocular pressure was not present (Supplementary Fig. S2, <http://www.iovs.org/cgi/content/full/50/1/242/DC1>).

It should be clarified that these abnormalities were primarily caused by ODAG overexpression or a secondary effect. To detect transgenic ODAG-expressing cells, we attached *IRE5/EGFP* to *ODAG* coding region as a reporter gene (Fig. 1A), which would enable us to identify transgenic ODAG-expressing cells by green fluorescence. Fluorescence analysis of the retina demonstrated that EGFP expression was high in the presumptive ONL, weak in the presumptive INL, and not detectable in the GCL (Fig. 4B), which is in good accordance with the results of previous reports of the mouse *Crx* promoter.<sup>5,6</sup> Since most of the layers in adult retina (OS, ONL, OPL, INL, and IPL) originated from the presumptive ONL and INL and their fibers, the impaired development of these layers would be the direct effect caused by deregulated ODAG expression. On the other hand, since ODAG was not expressed in the GCL, the reason that the GCL was also poorly developed remains unknown. Considering that ganglion cell development occurs by physically and functionally interacting with other types of cells existing in ONL and INL, such as photoreceptor cells, horizontal cells, bipolar cells, and amacrine cells,<sup>20</sup> it would be likely that deregulated expression of ODAG in the presumptive ONL and presumptive INL secondarily affected ganglion cells growth and consequently induced poor GCL development. In addition, since the optic nerve is the axonal neurite elongated from the GCL, the optic nerve atrophy observed in ODAG Tg may also be a secondary effect of overexpressed ODAG.

The mechanism underlying gradual eye protrusion with high ocular pressure is to be clarified. As shown in Figure 3B, since the anterior chamber angle was open in ODAG Tg as well as in WT, increased IOP was not attributable to a mechanical blockage of the aqueous humor outflow, thus indicating another mechanism. One possibility is that *Crx* promoter-mediated ODAG expression may induce dysregulated aqueous humor production. *Crx* promoter has been shown to drive transgene expression in photoreceptor cells.<sup>5,6</sup> In the embryonic stage, since photoreceptor and ciliary body cells originate from the same source, neural ectoderm, it would be possible that the *Crx* promoter induces ODAG overexpression in the ciliary body as well as photoreceptor cells. Since the ciliary body produces aqueous humor, it is possible that overexpressed ODAG in the ciliary body impairs regulation of aqueous humor production, with excessive aqueous humor causing ocular hypertension.

To investigate molecular mechanism(s) regulating the ODAG-mediated signaling pathway, we performed a GST-ODAG pull-down assay with mass spectrometry in retinal precursor cells and identified Rab6 and Rab6-GAP as recombinant ODAG-binding proteins (Fig. 5). Rab6 belongs to the group of small GTPase family proteins that trigger various cellular processes, including cell proliferation, differentiation, intracellular trafficking, membrane ruffling, and assembly of actin stress fibers.<sup>21-23</sup> Rab6 is localized in the Golgi complex and plays an important role in intra-Golgi transport.<sup>21,23</sup> In one study of the frog eye, Rab6 was reported to be a part of the sorting machinery of photoreceptors that delivers newly synthesized rhodopsin from the trans-Golgi to the site of the new rod outer segment,<sup>24,25</sup> and a subsequent study demonstrated that de-

fects in rhodopsin transportation in *Drosophila* induces retinal degeneration.<sup>26</sup> These results indicate that Rab6 plays an essential role in photoreceptor and retinal development through rhodopsin transportation.

Of interest, a recent study demonstrated that another small GTPase, Rab8, participates in vesicular transport<sup>27</sup> and is involved in the pathogenesis of human glaucoma.<sup>28</sup> Optineurin, whose mutations are found in a subset of patients with glaucoma,<sup>29</sup> is physically associated and functionally interacted with Rab8. On apoptotic stimuli, optineurin moves from the Golgi complex to the nucleus, and this subcellular translocation is dependent on the GTPase activity of Rab8. In addition, Rab6 and Rab8 were reported to function sequentially in rhodopsin transport and synergistically participate in rod outer segment disc morphogenesis.<sup>24</sup> These results suggest that aberrant expression of ODAG might impair Rab6/Rab6-GAP function, which eventually perturbs ocular homeostasis and consequently induces various abnormalities observed in ODAG Tg. Further studies are necessary to clarify the mechanism(s) of whether and how overexpressed ODAG affects functional properties of small GTPases, including Rab6.

The primary structure of mouse ODAG showed a zinc-finger domain at the N terminus, suggesting that ODAG may function as a transcription factor.<sup>4</sup> To address this possibility, we generated ODAG-EGFP fusion protein and investigated its subcellular localization. We found that ODAG-EGFP was mainly localized in the nucleus and partly in the cytoplasm (Supplementary Fig. S3, <http://www.iovs.org/cgi/content/full/50/1/242/DC1>), suggesting that ODAG may play a role as a nuclear protein as well as a Rab6/Rab6-GAP-interacting molecule, and possibly transport signals from the cytoplasm to the nucleus. Human counterpart of ODAG, which has a 92% amino acid identity with mouse ODAG, was reported and deposited as "GATA zinc finger domain containing 1 (GATAD1)".<sup>30</sup> Therefore, it would be intriguing to examine whether human ODAG/GATAD1 may be involved in human disease with ocular hypertension.

In this study, aberrant expression of ODAG in the eye induced ocular hypertension, optic nerve atrophy, and impaired retinal development, and Rab6-GAP and its substrate, Rab6, were found to be ODAG-associated proteins. These results indicate that physiologically controlled ODAG expression is essential for normal ocular development, possibly through a Rab6/Rab6-GAP-mediated signaling pathway. Our findings provide new insight into the mechanisms regulating ocular homeostasis and ODAG Tg would be a novel animal model for diseases that are caused by ocular hypertension.

### Acknowledgments

The authors thank Gail M. Seigel (University of Buffalo, New York) for providing us with the R28 retinal precursor cells.

### References

- Hill RE, Favor J, Hogan BL, et al. Mouse small eye results from mutations in a paired-like homeobox-containing gene. *Nature*. 1991;354:522-525.
- Mathers PH, Grinberg A, Mahon KA, Jamrich M. The Rx homeobox gene is essential for vertebrate eye development. *Nature*. 1997; 387:603-607.
- Furukawa T, Morrow EM, Cepko CL. *Crx*, a novel *otx*-like homeobox gene, shows photoreceptor-specific expression and regulates photoreceptor differentiation. *Cell*. 1997;91:531-541.
- Tsuruga T, Kanamoto T, Kato T, Yamashita H, Miyagawa K, Mishima HK. Ocular development-associated gene (ODAG), a novel gene highly expressed in ocular development. *Gene*. 2002; 290:125-130.
- Furukawa A, Koike C, Lippincott P, Cepko CL, Furukawa T. The mouse *Crx* 5'-upstream transgene sequence directs cell-specific

- and developmentally regulated expression in retinal photoreceptor cells. *J Neurosci*. 2002;22:1640-1647.
6. Nishida A, Furukawa A, Koike C, et al. Otx2 homeobox gene controls retinal photoreceptor cell fate and pineal gland development. *Nat Neurosci*. 2003;6:1255-1263.
  7. Miyazaki K, Kawamoto T, Tanimoto K, Nishiyama M, Honda H, Kato Y. Identification of functional hypoxia response elements in the promoter region of the DEC1 and DEC2 genes. *J Biol Chem*. 2002;277:47014-47021.
  8. Honda H, Oda H, Suzuki T, et al. Development of acute lymphoblastic leukemia and myeloproliferative disorder in transgenic mice expressing p210bcr/abl: a novel transgenic model for human Ph1-positive leukemias. *Blood*. 1998;91:2067-2075.
  9. Mabuchi F, Lindsey JD, Aihara M, Mackey MR, Weinreb RN. Optic nerve damage in mice with a targeted type I collagen mutation. *Invest Ophthalmol Vis Sci*. 2004;45:1841-1845.
  10. Kanamoto T, Mota M, Takeda K, et al. Role of apoptosis signal-regulating kinase in regulation of the c-Jun N-terminal kinase pathway and apoptosis in sympathetic neurons. *Mol Cell Biol*. 2000;20:194-204.
  11. Preobrazhenska O, Yakymovych M, Kanamoto T, et al. BRCA2 and Smad3 synergize in regulation of gene transcription. *Oncogene*. 2002;21:5660-5664.
  12. Kanamoto T, Hellman U, Heldin CH, Souchelnytskyi S. Functional proteomics of transforming growth factor-beta1-stimulated Mv1Lu epithelial cells: Rad51 as a target of TGFbeta1-dependent regulation of DNA repair. *EMBO J*. 2002;21:1219-1230.
  13. Seigel GM. Establishment of an E1A-immortalized retinal cell line. *In Vitro Cell Dev Biol*. 1996;32:66-68.
  14. Seigel GM, Sun W, Wang J, Hershberger DH, Campbell LM, Salvi RJ. Neuronal gene expression and function in the growth-stimulated R28 retinal precursor cell line. *Curr Eye Res*. 2004;28:257-269.
  15. Lindsey JD, Weinreb RN. Elevated intraocular pressure and transgenic applications in the mouse. *J Glaucoma*. 2005;14:318-320.
  16. John SW, Smith RS, Savinova OV, et al. Essential iris atrophy, pigment dispersion, and glaucoma in DBA/2J mice. *Invest Ophthalmol Vis Sci*. 1998;39:951-962.
  17. Libby RT, Anderson MG, Pang IH, et al. Inherited glaucoma in DBA/2J mice: pertinent disease features for studying the neurodegeneration. *Vis Neurosci*. 2005;22:637-648.
  18. Bayer AU, Neuhardt T, May AC, et al. Retinal morphology and ERG response in the DBA/2NNia mouse model of angle-closure glaucoma. *Invest Ophthalmol Vis Sci*. 2001;42:1258-1265.
  19. Aihara M, Lindsey JD, Weinreb RN. Ocular hypertension in mice with a targeted type I collagen mutation. *Invest Ophthalmol Vis Sci*. 2003;44:1581-1585.
  20. Harada T, Harada C, Parada LF. Molecular regulation of visual system development: more than meets the eye. *Genes Dev*. 2007;21:367-378.
  21. Goud B, Zahraoui A, Tavitian A, Saraste J. Small GTP-binding protein associated with Golgi cisternae. *Nature*. 1990;345:553-556.
  22. Ridley AJ, Hall A. The small GTP-binding protein rho regulates the assembly of focal adhesions and actin stress fibers in response to growth factors. *Cell*. 1992;70:389-399.
  23. Tisdale EJ, Bourne JR, Khosravi-Far R, Der CJ, Balch WE. GTP-binding mutants of rab1 and rab2 are potent inhibitors of vesicular transport from the endoplasmic reticulum to the Golgi complex. *J Cell Biol*. 1992;119:749-761.
  24. Deretic D, Papermaster DS. Rab6 is associated with a compartment that transports rhodopsin from the trans-Golgi to the site of rod outer segment disk formation in frog retinal photoreceptors. *J Cell Sci*. 1993;106.
  25. Deretic D. Post-Golgi trafficking of rhodopsin in retinal photoreceptors. *Eye*. 1998;12:526-530.
  26. Shetty KM, Kurada P, O'Tousa JE. Rab6 regulation of rhodopsin transport in Drosophila. *J Biol Chem*. 1998;273:20425-20430.
  27. Zerial M, McBride H. Rab proteins as membrane organizers. *Nat Rev Mol Cell Biol*. 2001;2:107-117.
  28. De Marco N, Buono M, Troise F, Diez-Roux G. Optineurin increases cell survival and translocates to the nucleus in a Rab8-dependent manner upon an apoptotic stimulus. *J Biol Chem*. 2006;281:16147-16156.
  29. Rezaie T, Child A, Hitchings R, et al. Adult-onset primary open-angle glaucoma caused by mutations in optineurin. *Science*. 2002;295:1077-1079.
  30. Strausberg RL, Feingold EA, Grouse LH, et al. Generation and initial analysis of more than 15,000 full-length human and mouse cDNA sequences. *Proc Natl Acad Sci USA*. 2002;99:16899-16903.